SUPPLEMENTAL INFORMATION

James Chen[1], Brandon Malone[1], Eliza Llewellyn[1], Michael Grasso[2], Patrick M. M. Shelton[2], Paul Dominic B. Olinares[3], Kashyap Maruthi[4], Ed Eng[4], Hasan Vatandaslar[5], Brian T. Chait[3], Tarun Kapoor[2], Seth A. Darst[1] Elizabeth A. Campbell[1]

[1]Laboratory of Molecular Biophysics, The Rockefeller University, New York, NY, 10065 USA.

[2]Laboratory of Chemistry and Cell Biology, The Rockefeller University, New York, NY, 10065 USA.

[3]Laboratory of Mass Spectrometry and Gaseous Ion Chemistry, The Rockefeller University, New York, NY, 10065 USA.

[4]The National Resource for Automated Molecular Microscopy, Simons Electron Microscopy Center, New York Structural Biology Center, New York, NY, 10027 USA.

[5]Institute of Molecular Health Sciences, ETH Zurich, 8093 Zürich, Switzerland.

Supplemental information includes 6 figures and 1 table.

Table S1 | Cryo-EM data collection, refinement and validation statistics. Related to Figure 2.

Dataset	**nsp13-RTC (CHAPSO)**		
Sample ID	$nsp13_1$-RTC	$nsp13_2$-RTC	$(nsp13_2\text{-RTC})_2$
EMDB		EMD-22160	
PDB		6XEZ	
Data collection and processing			
Microscope	FEI Titan Krios	FEI Titan Krios	FEI Titan Krios
Voltage (kV)	300	300	300
Detector	Gatan K3	Gatan K3	Gatan K3
Electron exposure (e–/Å2)	64	64	64
Defocus range (μm)	-0.8 to -2.5	-0.8 to -2.5	-0.8 to -2.5
Data collection mode	Counting Mode	Counting Mode	Counting Mode
Nominal Magnification	81,000x	81,000x	81,000x
Pixel size (Å)	1.1	1.1	1.1
Symmetry imposed	C1	C1	C1
Initial particle images (no.)	1447307	1447307	1447307
Final particle images (no.)	17345	58942	11771
Map resolution (Å) - FSC threshold 0.143	4.0	3.5	7.9
Map resolution range (Å)	3.2-7.6	2.8-7.1	4.0-10.3
Refinement			
Initial model used (PDB code)		6YYT/6JYT	
Map sharpening B factor (Å2)	-60.7	-76.8	-417.7
Model composition			
Non-hydrogen atoms		21,744	
Protein residues		2,563	
Nucleic acid residues (RNA)		70	
Ligands		8 Zn^{2+}, 3 Mg^{2+}, 3 CHAPSO, 3 ADP, 2 AF_3	
B factors (Å2)			
Protein		50.08	
Nucleic acid		75.64	
Ligands		89.8	
R.m.s. deviations			
Bond lengths (Å)		0.01	
Bond angles (°)		0.945	
Validation			
MolProbity score		3.20	
Clashscore		19.89	

Poor rotamers (%)	10.77
Ramachandran plot	
Favored (%)	86.91
Allowed (%)	13.01
Disallowed (%)	0.08

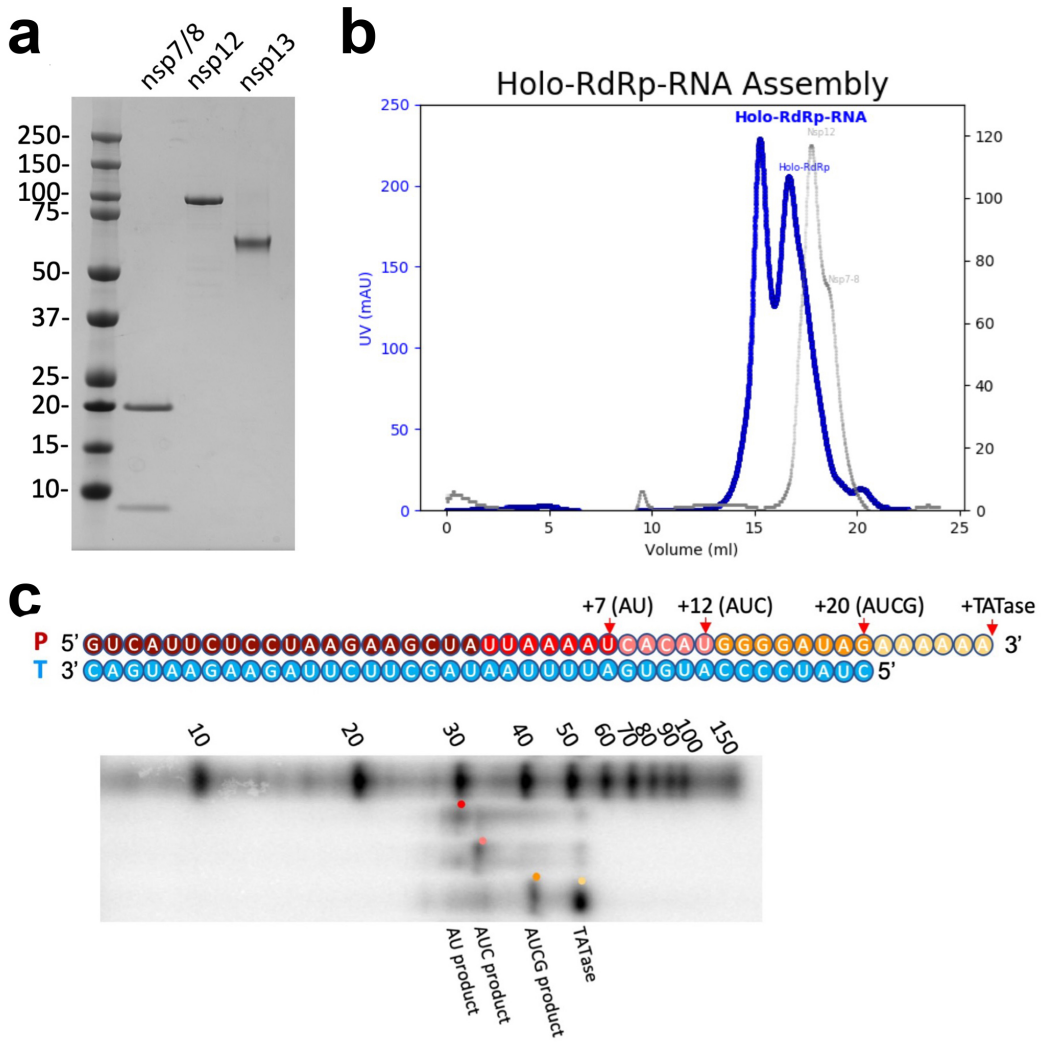

Figure S1

Figure S1. Purification and assembly of nsp13 and the RTC. Related to Figure 1.

a. SDS-PAGE of purified SARS-CoV-2 nsp7/8, nsp12, and nsp13.

b. Purification of RTC by size exclusion chromatography.

(left) Chromatogram of RTC (blue trace) and individual components (grey trace) labeled.

c. Holo-RdRp elongates the primer-strand of the RNA scaffold shown in the presence of NTPs. Original primer (20mer, dark red), 27mer AU elongated product (red), 32mer AUC product (pink), 40mer AUCG product (orange) and the product of nsp8-mediated TATAse activity [yellow; (Tvarogová et al., 2019). Products, taken at a 30 minute timepoint, are shown for a representative gel (n=2) and are visualized alongside Decade RNA ladder (Invitrogen).

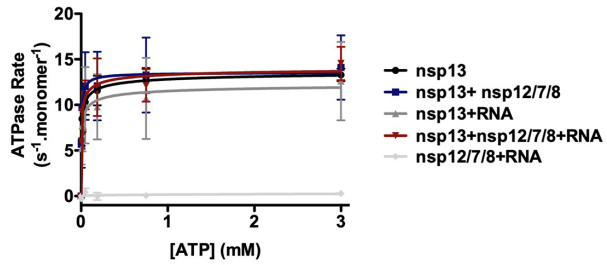

	K_{cat} (s^{-1})	K_m (μM)
Nsp13	13.97	4.80
Nsp13 + Nsp12/7/8	13.56	4.12
Nsp13 + RNA	12.59	5.02
Nsp13 + Nsp12/7/8 + RNA	14.29	4.47
Nsp12/7/8 + RNA	N/A	N/A

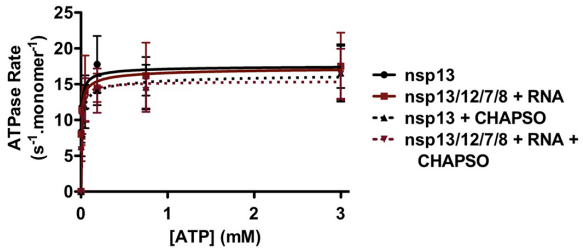

	K_{cat} (s^{-1})	K_m (μM)
Nsp13	17.65	3.70
Nsp13 + Nsp12/7/8 + RNA	17.62	3.77
Nsp13 + CHAPSO	16.81	6.61
Nsp13 + Nsp12/7/8 + RNA + CHAPSO	15.49	5.17

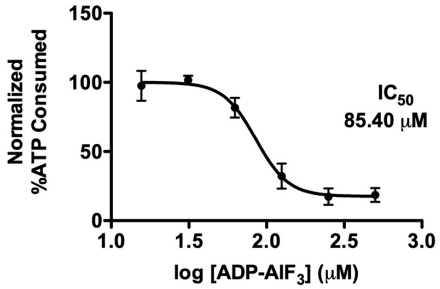

Figure S2. Nsp13 activities. Related to Figure 1.

a. *(left)* ATPase assay comparing nsp13 alone, nsp13 + holo-RdRp (nsp12/7/8), nsp13 + RNA scaffold alone, nsp13-RTC (nsp13/12/7/8 + RNA), and the RTC alone (nsp12/7/8 + RNA). Error bars indicate the range for two independent measurements.

(right) Calculated K_{cat} and K_m values for the ATPase assay.

b. *(left)* ATPase assay comparing nsp13 alone and nsp13-RTC (nsp13/12/7/8 + RNA) ± 8 mM CHAPSO. Error bars indicate the range for two independent measurements.

(right) Calculated K_{cat} and K_m values for the ATPase assay.

c. Inhibitory effect of ADP-AlF_3 on nsp13 ATPase activity (N=6). Error bars denote standard deviation.

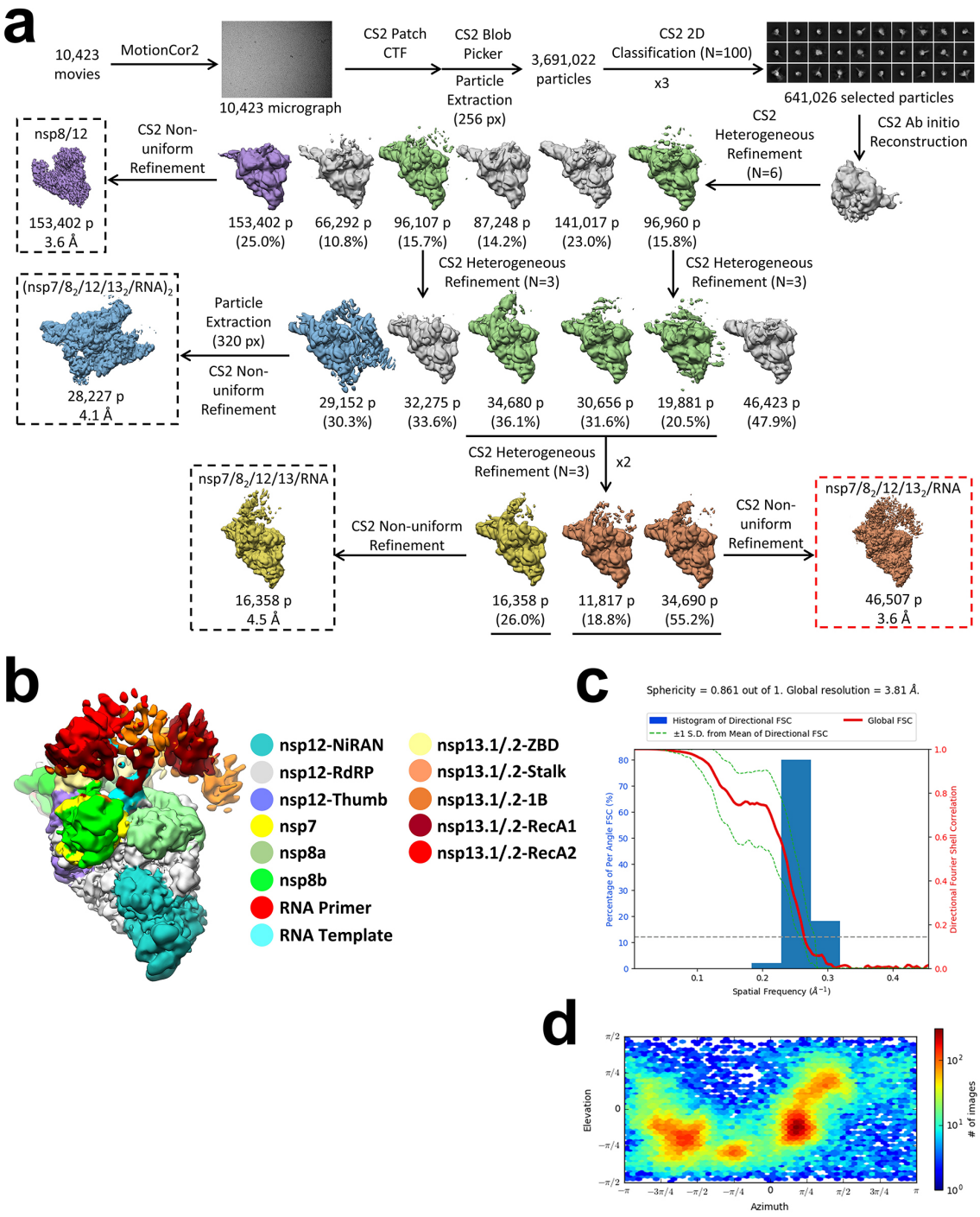

Figure S3

Figure S3. Cryo-EM processing pipeline and analysis for nsp13-RTC (no detergent) dataset. Related to Figure 2.

a. Cryo-EM processing pipeline.

b. Nominal 3.6 Å-resolution cryo-EM reconstruction of $nsp13_2$-RTC (no detergent) filtered by local resolution (Cardone et al., 2013) and colored by subunit according to the key on the right.

c. Directional 3D Fourier shell correlation (FSC) for $nsp13_2$-RTC (no detergent) calculated by 3DFSC (Tan et al., 2017).

d. Angular distribution plot for reported $nsp13_2$-RTC (no detergent) calculated in cryoSPARC. Scale shows the number of particles assigned to a particular angular bin. Blue, a low number of particles; red, a high number of particles.

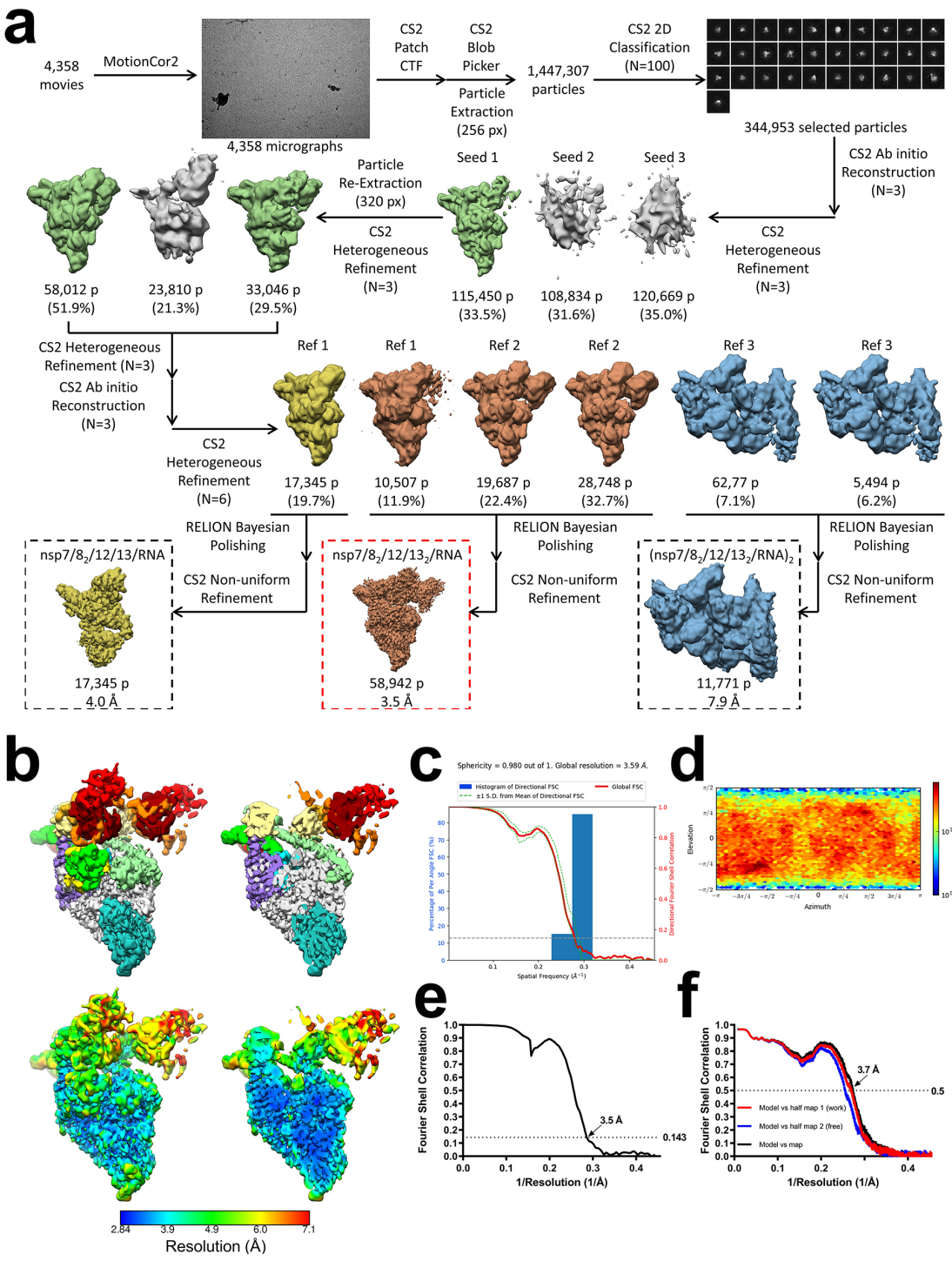

Figure S4

Figure S4. Cryo-EM processing pipeline and analysis for nsp13-RTC (CHAPSO) dataset. Related to Figure 2.

a. Cryo-EM processing pipeline.

b. Nominal 3.5 Å-resolution cryo-EM reconstruction of $nsp13_2$-RTC (CHAPSO) filtered by local resolution (Cardone et al., 2013). The view on the right is a cross-section.

(top) Colored by subunit.

(bottom) Color by local resolution (key on the bottom).

c. Directional 3D Fourier shell correlation (FSC) for $nsp13_2$-RTC (CHAPSO) calculated by 3DFSC (Tan et al., 2017).

d. Angular distribution plot for reported $nsp13_2$-RTC (CHAPSO) calculated in cryoSPARC. Scale shows the number of particles assigned to a particular angular bin. Blue, a low number of particles; red, a high number of particles.

e. Gold-standard FSC plot for $nsp13_2$-RTC (CHAPSO), calculated by comparing two independently determined half-maps from cryoSPARC. The dotted line represents the 0.143 FSC cutoff which indicates a nominal resolution of 3.5 Å.

f. FSC calculated between the refined structure and the half map used for refinement (work, red), the other half map (free, blue), and the full map (black).

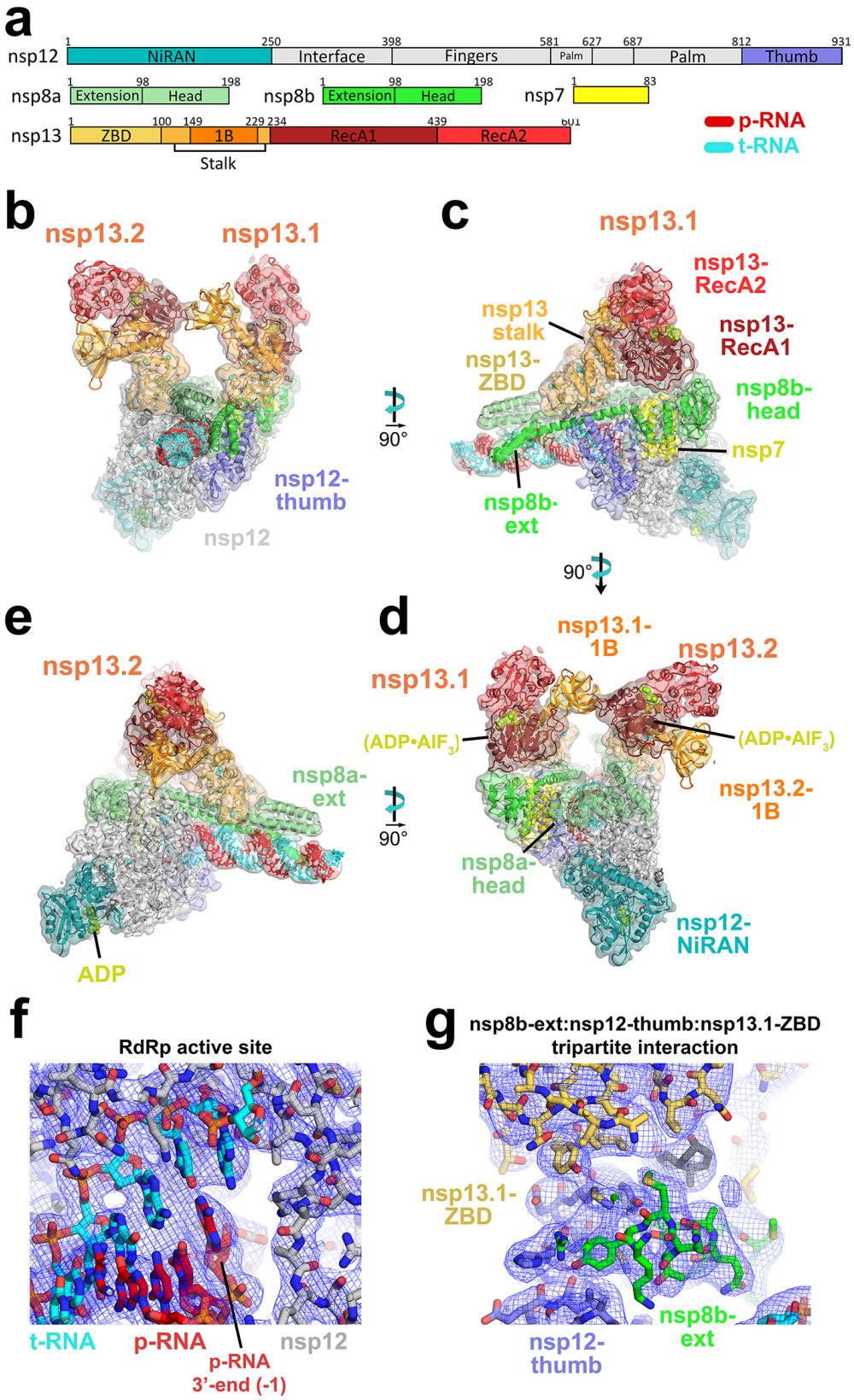

Figure S5

Figure S5. Cryo-EM density maps. Related to Figure 2.

a. Schematic illustrating domain structure of SARS-CoV-2 holo-RdRp (nsp7, nsp8, nsp12) and nsp13. The color-coding corresponds to the figures throughout this manuscript unless otherwise specified.

b-e. Orthogonal views showing the overall architecture of the $nsp13_2$-RTC. Shown is the transparent cryo-EM density (local-resolution filtered) with the $nsp13_2$-RTC model superimposed. Same views as Figure 2b-e.

f. View of the nsp12 (RdRp) active site (refined model superimposed onto the cryo-EM density, shown as blue mesh), showing the post-translocated state of the RNA.

g. View of the nsp8b-extenstion:nsp12-thumb:nsp13-ZBD tripartite interaction (refined model superimposed onto the cryo-EM density, shown as blue mesh). Similar view as Figure 3a.

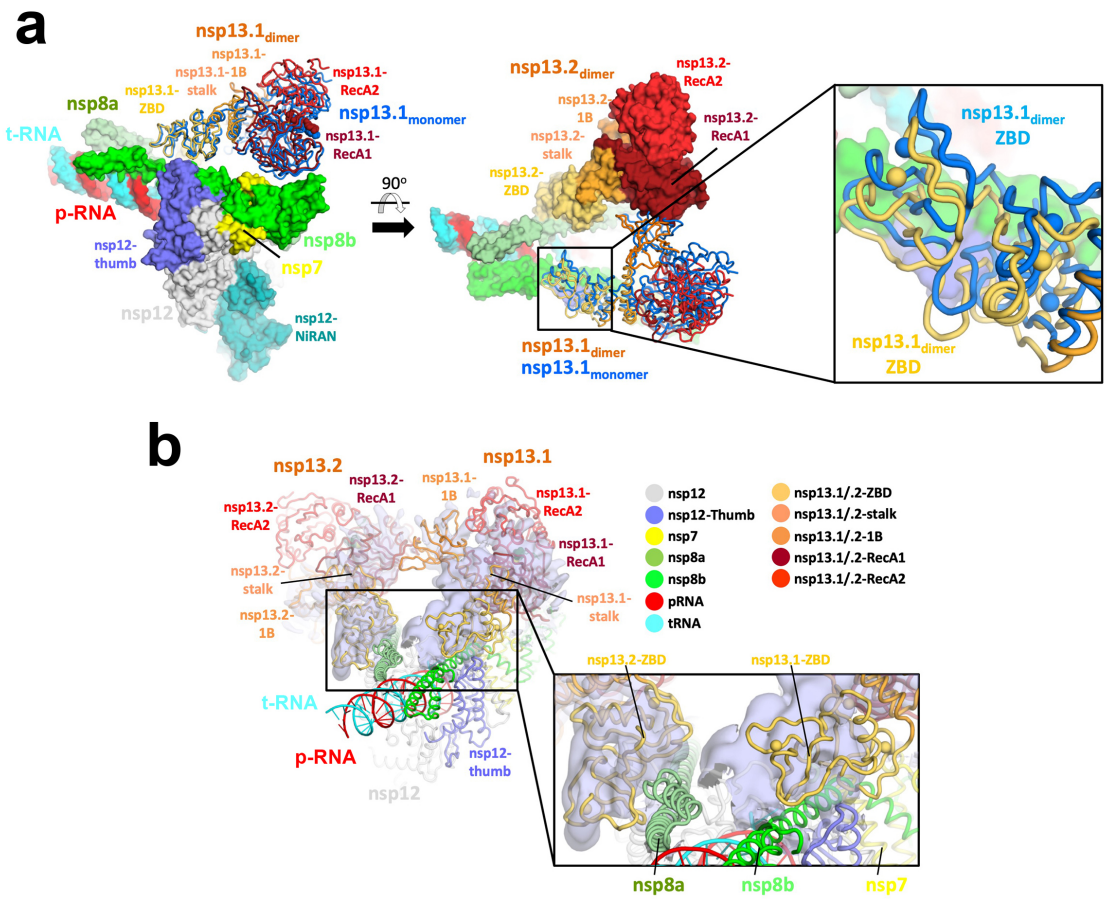

Figure S6

Figure S6. Comparison of nsp13$_2$-RTC (CHAPSO) structure with nsp13$_1$-RTC (CHAPSO) and nsp13$_2$-RTC (no detergent). Related to Figure 3.

a. Structure of nsp13$_2$-RTC (CHAPSO) colored according to key in **b** and shown as a molecular surface except nsp13.1, which is shown as cartoon tubes. Superimposed on the overall structure is nsp13 (marine) modeled from the nsp13$_1$-RTC (CHAPSO). Overall RMSD (calculated using 'rms_cur' in PyMOL) between the two nsp13.1 structures is 8.1 Å over 596 Cα atoms. (left) overall structure. (middle) overall structure rotated 90°. (right) zoom-in of boxed region in middle panel, showing region around nsp13.1-ZBD.s RMSD (calculated using 'rms_cur' in PyMOL) between the two nsp13.1 ZBDs is 3.6 Å over 100 Cα atoms.

b. Structure of nxp13$_2$-RTC (CHAPSO) is shown in cartoon tubes, colored based on key, and superimposed onto the cryo-EM map from the nsp13$_2$-RTC (no detergent) dataset (shown as light blue transparent surface). Density map is locally filtered by resolution and difference density for nsp13 is highlighted using 'isosurf' command in PyMOL with 10 Å carve buffer. (left) overall structure. (right) zoom-in of boxed region in left panel, showing region around nsp13-ZBDs.